Renewable and Sustainable Energy Reviews 41 (2015) 1028–1036

Contents lists available at ScienceDirect

Renewable and Sustainable Energy Reviews

journal homepage: www.elsevier.com/locate/rser

Thermal transmittance of carbon nanotube networks: Guidelines for novel thermal storage systems and polymeric material of thermal interest

Matteo Fasano, Masoud Bozorg Bigdeli, Mohammad Rasool Vaziri Sereshk, Eliodoro Chiavazzo, Pietro Asinari *

Energy Department, Politecnico di Torino, Corso Duca degli Abruzzi 24, Turin 10129, Italy

ARTICLE INFO

Article history:
Received 17 October 2013
Received in revised form
25 August 2014
Accepted 30 August 2014

Keywords:
Thermal storage
Thermal boundary resistance
Thermal conductivity
Polymeric heat exchangers
Carbon nanotube networks
Composite materials

ABSTRACT

Among other applications, the study of thermal properties of large networks of carbon nanoparticles may have a critical impact in *loss-free*, more compact and efficient thermal storage systems, as well as thermally conducting polymeric materials for innovative low-cost heat exchangers. In this respect, here, we both review and numerically investigate the impact that nanotechnology (and in particular carbon-based nanostructures) may have in the near future. In particular, we focus on the role played by some geometrical and chemical parameters on the overall thermal transmittance of large complex networks made up of carbon nanotubes (CNTs), that can be potentially added as fillers to (thermally) low-conductive materials for enhancing the transport properties. Several configurations consisting of sole and pairs of single-walled carbon nanotubes (SWCNTs) and double-walled carbon nanotubes (DWCNTs), characterized by different dimensions and number of C–O–C interlinks, are considered. Based on the results found in the literature and using focused simulations using standard approaches in Non-Equilibrium Molecular Dynamics (NEMD), we highlight the dependence on the particle diameter, length, overlap and functionalizations of both thermal conductivity and boundary resistance across CNTs, which are indeed the relevant quantities for obtaining composite materials with desired unusual thermal properties. We observe that CNTs with short overlap length and a few interlinks already show a remarkable enhancement in the overall transmittance, whereas further increase in the number of C–O–C connections only carries marginal benefits. We believe that much understanding has been gained so far in this field thanks to the work of chemists and material scientists, thus it is time to draw the attention of engineers active in the energy sector and thermal scientists on such findings. Our effort, therefore, is to gather in this article some guidelines towards innovative thermal systems that may be manufactured and employed in the near future for addressing a great challenge of our society: Storage and use of thermal energy.

Contents

* Corresponding author.
E-mail address: pietro.asinari@polito.it (P. Asinari).

http://dx.doi.org/10.1016/j.rser.2014.08.087
1364-0321/

1. Introduction

Thermal energy storage for sufficiently long periods is known to be a critical issue in thermal sciences. In general, nanotechnology (and particularly carbon based nanostructures) may hold the premise for successfully addressing energy issues in modern society [1,2].

In particular, recently, an innovative system with the capacity of storing thermal energy potentially for an indefinite time have attracted much attention thanks to the pioneering work of scientists at the Fraunhofer Institute for Interfacial Engineering and Biotechnology, together with ZeoSys GmbH [3]. In addition, such a new technology can store three to four times more energy compared to water based systems. The new system contains zeolite pellets and one of the key challenge here is (i) to ensure optimal heat transfer (high overall conductivity) through the zeolites during the thermal loading and (ii) to allow water percolation during the thermal release, in the same device. The latter competing (and extreme) features may be met by dispersing highly conductive materials (fillers) within the zeolite pellets (matrix) [4].

The use of carbon-based nanoparticles (e.g. carbon nanotubes, graphene, etc.) certainly represents one of the most promising alternative. On the other hand, even for perfectly dispersed fillers forming an ideal percolating network, realizing a sufficiently high thermal transmittance for the overall network is everything but a simple task. In fact, typically high thermal resistances are experienced by the heat flux across the several interfaces characterizing such composite materials (see e.g. [5,6]). It is therefore highly desirable to systematically investigate on the several mechanisms that contribute to the value of the overall thermal transmittance of such complex percolating networks. Moreover, those studies have a critical impact also on polymeric materials for innovative heat exchangers and other composite materials [7–10].

Since their first observation by Iijima [11], Carbon Nanotubes (CNTs) have attracted an increasing attention because of their outstanding physical properties. In fact, superior mechanical, electric and (most importantly) thermal properties of CNTs have been reported [12], and this certainly makes such material a versatile building block for future engineering applications [13].

Among others, thermal properties of CNTs have been widely investigated in recent years, both experimentally and theoretically [14,15]. For instance, pristine CNTs are characterized by one of the largest value of thermal conductivity, ranging from 2400 $W\,m^{-1}\,K^{-1}$ to 4740 $W\,m^{-1}\,K^{-1}$ depending on the experimental conditions [14]. Moreover, thermal conductivity of CNTs may be tuned by introducing defects, vacancies, surface functionalizations or junctions [16,17], thus allowing the design of CNT-based composite materials with desired enhanced thermal properties [18,19]. CNT-based composites are typically made out of polymeric, ceramic or metallic matrices and carbon-based fillers, such as CNTs, graphene or carbon nanoribbons [20,21].

CNTs spontaneously tend to bundle and cross-link each other because of their high intermolecular cohesive forces [22], whereas precise geometries of CNT networks can be induced by means of proper chemical functionalizations [23]. Therefore, CNT networks are energetically and thermodynamically stable up to 600 K, and CNTs synthetized within a polymeric or ceramic matrix can exist in a stable and designable cross-linked form [24]. Due to their peculiar thermal and technological properties, CNT fillers have been employed in a promising variety of applications, such as thermal interface material [25–27], electrical interconnects [28], electronic nanocircuits [29], triggered drug release [30], artificial muscles [31], thermal nanocircuits [32–34], nanofluids for heat transfer [35–37], energy harvesting [38] and gas or thermal storages [24,39]. For example, CNT networks are promising technological solutions for improving the internal distribution of heat within thermal storage applications, such as nanoporous zeolite devices, in order to reach a better control and efficiency of the heat accumulation/release cycle [40]. In the latter case, CNT networks need to be engineered and properly designed for reducing thermal losses at low filling ratio in the matrix. However, experimental benchmarks and molecular simulations of carbon-based networks reveal an overall thermal performance lower than expected, which is mainly due to CNT–CNT and CNT–matrix thermal boundary resistances [41–44].

It is well known that heat conduction by CNTs is predominantly a phononic phenomenon (i.e. coupled vibration of carbon atoms), rather than an electronic one [45]. The reasons for high thermal conductivity of CNTs are due to their large speed of sound, long range crystallinity and long phonon mean free path [14,46]. Nevertheless, the bottleneck of heat transfer within carbon-based networks is the thermal boundary resistance (also known as Kapitza resistance), which defines the thermal impedance between different materials. Kapitza resistance is generated by phonon scattering, which produces a local temperature discontinuity in heat transfer phenomena at the nanoscale. Vacancies, functionalizations, defects as well as interfaces between different materials (solid or liquid) contribute to thermal boundary resistance [47–55]. Therefore, the difference between intertube and intratube thermal conduction, which can also be orders of magnitude, limits the overall thermal transmittance of the CNT-based composites. Hence, a better understanding of the geometry, chemistry and arrangement of CNT networks is needed, in order to have guidelines in designing composite materials with desired heat transfer performances. Recent studies about carbon-based composite materials show that a better efficiency in heat transfer is achieved when CNTs percolate within the matrix, creating a homogeneous and cross-linked network [6,56,57]. Owing to the current experimental difficulties in synthetizing high quality and well-ordered CNTs, computational studies have been conducted to systematically analyze the thermal properties of CNT and CNT networks [57–60]. Among others, Molecular Dynamics (MD) simulations have been widely used for improving the physical understanding and predicting the thermal transport in carbon-based composite materials [61]. In this study, thermal properties of CNTs with different diameter, length, chirality, number of walls, overlap and chemical functionalization are investigated by means of MD simulations. Hence, this work aims at systematically reporting and analyzing the geometrical and chemical parameters affecting the thermal conductivity and the thermal boundary resistance of CNT networks, in order to come up with a few general guidelines for designing the overall thermal transmittance of CNT-based composites.

2. Materials and methods

Non-Equilibrium Molecular Dynamics (NEMD) simulations are performed for estimating the thermal conductivity λ of CNTs and the thermal boundary resistance R_k between adjacent CNTs. The latter configuration can be regarded as the building block of large

and complex carbon-based networks as those of interest in today nanofluids and composite material [5,7,62].

Thermal properties of Single-Walled Carbon Nanotubes (SWCNTs, Fig. 1a) and Double-Walled Carbon Nanotubes (DWCNTs, Fig. 1b), which are composed by two coaxial SWCNTs, are investigated in different setups, ranging from a sole CNT to larger CNT aggregates. First of all, the effect of the CNT geometry on thermal conductivity is investigated. In particular, in our simulations we choose (i) CNT with diameters of 0.7, 1.4, 4.5 and 5.0 nm; (ii) CNT with length of 10, 20, 30 and 40 nm; (iii) CNT with different chirality, namely armchair (*m*,*m*), chiral (*m*,*n*) or zigzag (*m*,0). Second, the effect of tube overlap (ranging from 0% to 100% of the CNT length) and chemical bonding (0–8 C–O–C joints between parallel CNTs, Fig. 1c and d) on thermal boundary resistance between contiguous CNTs is explored.

In our simulations, the reciprocal orientation between the CNTs jointed by oxygen atoms is initialized according to C–O–C bond structure (Fig. 1e, C–O bonds are 1.43 Å long, C–O–C angle 109.5° wide) [63], while two types of interactions are taken into account: (i) the bonded interactions modeled as harmonic stretching and angle potentials, whereas the Rickaert–Bellemans potential is used for proper dihedral angles; (ii) non-bonded interactions accounting for the Van der Waals forces and modeled as a 12-6 Lennard–Jones potential with a shifted cut-off function (1.2 nm cut-off distance). All details on the employed force-field parameters are reported elsewhere [5,62–65].

The equations of motion are solved by a leap-frog algorithm with time step of $\Delta t = 0.5$ fs; whereas periodic boundary conditions along *x*,*y*,*z* directions are imposed. Upon energy minimization, the system is initialized at 300 K (Maxwellian distribution of velocities) and coupled to a Berendsen thermostat for 50 ps, until system's energies relax to a steady state. Afterwards, the NEMD approach is used for evaluating the thermal properties of CNT or CNT network [66]. A temperature gradient is induced in the CNT (or in the CNT network) by means of two Nosé–Hoover thermostats [67,68] ($T_1 = 280$ K; $T_2 = 320$ K) attached to the carbon atom rings at their ends (Figs. 1a–d). Thermostats are introduced in different positions according to the thermal properties to be evaluated. For example, in the DWCNT setup in Fig. 1b the green dotted thermostated carbon rings are employed for evaluating λ of the outer CNTs, whereas the red ones are used for λ of the inner one. Instead, in the case of overlapping SWCNTs depicted in Fig. 1c the green dotted thermostated carbon rings are employed for evaluating λ of the lower SWCNT, whereas the red ones for calculating the interlayer Kapitza resistance between the SWCNTs. The amount of atoms in the canonical ensemble (NVT) is optimized for obtaining constant heat flux and convergent values of λ in the simulated setups, and it is properly scaled according to the system size [69]; the remaining atoms are in the microcanonical ensemble (NVE). After the energy minimization, the first and the last rings of carbon atoms are restrained, in order to have fixed boundary conditions (Figs. 1a–d) [70]. NEMD simulations are continued up to 4 ns (depending on the system size). Temperature profiles and (Nosé–Hoover) friction factors [5,67–69] are then extracted from the simulated trajectories, in order to evaluate temperature gradient and specific heat flux in the NVE region, respectively [5]. Steady state is reached when the thermal conductivity λ and boundary resistance R_k (evaluated every 200 ps) tend to an asymptotic value; this is typically achieved after half of the simulation time has elapsed. Finally, λ and R_k values are evaluated over a data range of at least 500 ps once steady state is achieved, and checked for energy fluctuations.

All simulations are performed using the software package GROMACS [71], while picture rendering is accomplished using UCSF Chimera [72].

3. Theoretical background: Thermal transmittance of carbon nanotube networks

Thermal conduction in CNT-based composites (e.g. carbon fillers dispersed within a polymeric and/or ceramic matrix) is mainly affected by the mechanism of heat diffusion (i) through CNTs, (ii) between the CNTs in a CNT network, (iii) between the CNT network and the matrix, and (iv) through the matrix. Heat insulation or heat conduction enhancement in carbon-based composite materials can be influenced by varying the amount (and type) of cross-interactions as well as the arrangement of the CNTs within a network, such as choosing between randomly oriented

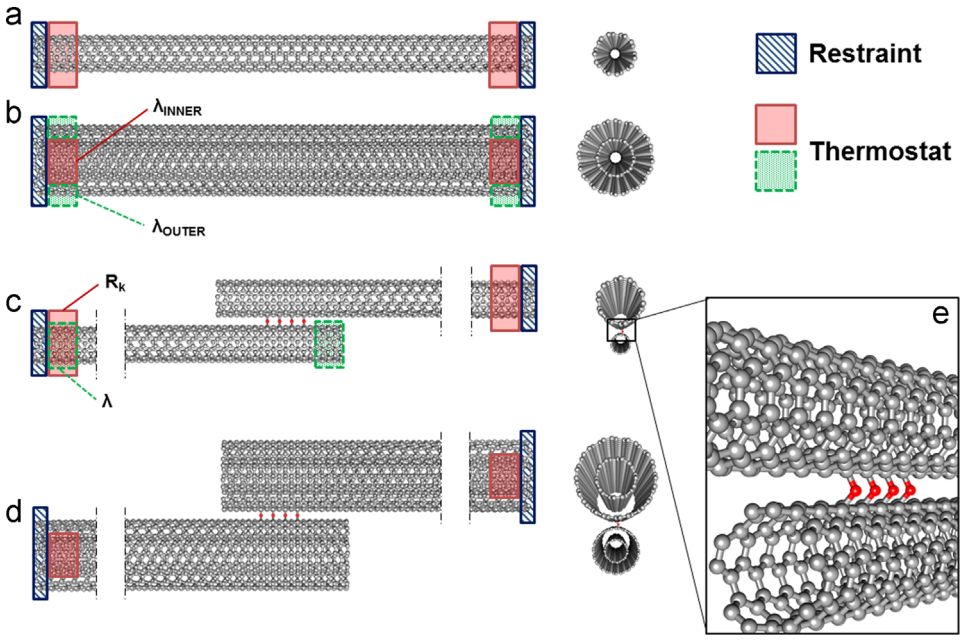

Fig. 1. Setups considered in the computations: (a) single-walled carbon nanotube; (b) double-walled carbon nanotube; (c) a pair of overlapping SWCNTs connected by 4 C–O–C covalent bonds (links); (d) a pair of overlapping DWCNTs connected by 4 C–O–C covalent bonds (links); and (e) detail of C–O–C joints. (For interpretation of the references to color in this figure, the reader is referred to the web version of this article.)

CNTs or aligned ones [14]. The aim of the present study is to systematically investigate the more fundamental aspects (i.e. at those acting at the nanoscale level) involved in the conductive heat transfer for the above setup.

Following a standard approach in the macroscopic heat transfer phenomena, the specific heat flux φ generated by a temperature difference ΔT within a CNT network can be defined as

$$\varphi = u\,\Delta T, \tag{1}$$

where the specific thermal transmittance u can be evaluated as

$$\frac{1}{u} = \sum_i \frac{L_i}{\lambda_i} + \sum_{i,j} R_{k,ij} + \sum_n R_{k,n}, \tag{2}$$

with λ_i being the thermal conductivity of the ith CNT (with length L_i); $R_{k,ij}$ the thermal boundary resistance between ith and jth CNTs; $R_{k,n}$ the nth thermal boundary resistance between the CNT network and a matrix [73,74], which is here considered just in series for the sake of simplicity (not investigated in this work).

More specifically, the present MD simulations aim at evaluating λ_i and $R_{k,ij}$, which are critical for the accurate estimate of the overall thermal transmittance in CNT networks of increasing complexity. Here, we focus on (i) sole SWCNT (Fig. 2a), where $1/u = L/\lambda$, L is the nanotube length and λ its thermal conductivity; (ii) sole DWCNT (Fig. 2b), where $1/u \cong L((1/\lambda_{in}) + (1/\lambda_{out})) + R_k$ in the specific setup here considered (heat flows from the leftmost end of the inner CNT to the rightmost end of the outer CNT), λ_{in} and λ_{out} are thermal conductivities of the inner and outer CNTs, respectively, and R_k is the Kapitza resistance between the layers; (iii) two adjacent SWCNTs (Fig. 2c), where $1/u = (L_1/\lambda_1) + R_{k,12} + (L_2/\lambda_2)$ and $R_{k,12}$ is the Kapitza resistance between the SWCNTs; (iv) two adjacent DWCNTs (Fig. 2d), where $1/u \cong [L_1((1/\lambda_{1,in}) + (1/\lambda_{1,out})) + R_{k,1}] + R_{k,12} + [L_2((1/\lambda_{2,in}) + (1/\lambda_{2,out})) + R_{k,2}]$ in the analyzed configuration (heat flows from the leftmost inner CNT to the rightmost inner CNT). In the latter case, $\lambda_{1,in}$ and $\lambda_{1,out}$ are the inner and outer thermal conductivities of the top DWCNT; $\lambda_{2,in}$ and $\lambda_{2,out}$ are the inner and outer thermal conductivities of the lower DWCNTs; $R_{k,1}$ and $R_{k,2}$ are defined as the intralayer Kapitza resistances in the DWCNTs and $R_{k,12}$ is the interlayer Kapitza resistance between the DWCNTs. Clearly, different heat paths within the network may imply different estimates of $1/u$. The above formulas are reported here only with the purpose to better highlight the dependence of u on the most relevant quantities to be investigated below.

4. Results

4.1. Thermal conductivity of carbon nanotubes

A first set of simulations has been performed for systematically assessing how geometrical, chemical and physical factors affect thermal conductivity of SWCNTs. Moreover, the adopted MD setup and force-field parameters have been validated by comparing the obtained trends for thermal conductivity with experimental and computational works published in the literature.

According to the NEMD approach, thermal conductivity is measured by means of the Fourier's law:

$$\lambda = -\frac{\varphi}{\partial T/\partial x}, \tag{3}$$

where $\varphi = \Phi/S$, with Φ being the steady state heat flux between two thermostated regions flowing across the tube cross-section S. Starting from the initial state, where the carbon rings at CNT ends are thermostated at 320 and 280 K respectively, while the remaining rings are equilibrated at 300 K, the temperatures of internal carbon rings tend to a steady state in a few ps (Fig. 3). The slope of time averaged temperature profile $\partial T/\partial x$ is measured along the x-axis of the nanotube in the region not attached to thermostats (Fig. 3). Different ways of computing S can be found in the literature, which significantly affect the absolute values of λ. Here, the cross-sectional area is intended as

$$S = 2\pi r b, \tag{4}$$

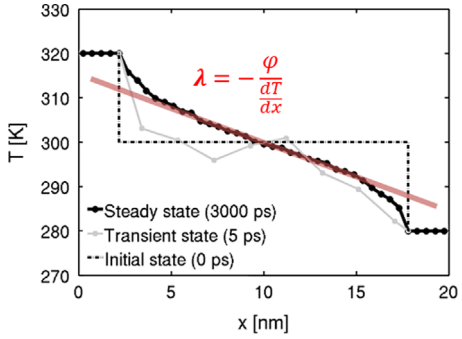

Fig. 3. NEMD approach for evaluating thermal conductivity λ of CNTs by means of Fourier's Law.

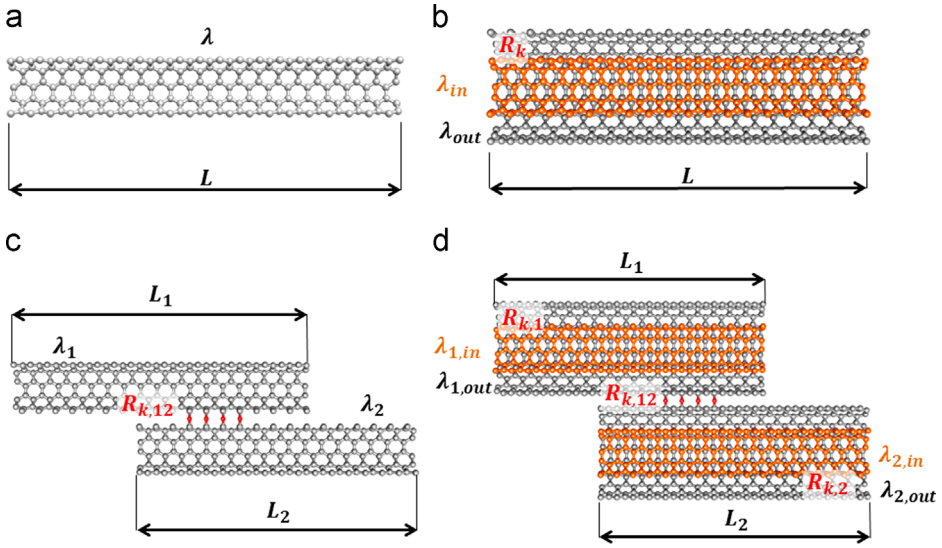

Fig. 2. Quantities appearing in the calculation of thermal transmittance in the studied setups: (a) SWCNT, (b) DWCNT, (c) a pair of overlapping SWCNTs connected by 4 C–O–C covalent bonds, and (d) a pair of overlapping DWCNTs connected by 4 C–O–C covalent bonds.

where r is the CNT radius where thermostat (i.e. the heat flux) is applied and $b = 0.34$ nm is the Van der Waals thickness of carbon atoms [75].

(10,10) SWCNT and (5,5) SWCNT, with length of 10 nm, are considered as benchmarks for validating the present MD results (Fig. 1a): The measured thermal conductivities (78 W m^{-1} K^{-1} and 75 W m^{-1} K^{-1}, respectively) are in good agreement with other results found in the literature for same setups. For example, Alaghemandi et al. measured 79 and 69 W m^{-1} K^{-1}, respectively [32]. Moreover, we found that restraints on carbon rings at the SWCNT ends (blue area in Fig. 1a) have negligible effects on λ, being 76 W m^{-1} K^{-1} the measured thermal conductivity of (5,5) SWCNT 10 nm long with free ends. It is well known that thermal conductivity of CNTs computed by the MD simulations can be orders of magnitude lower than the experimental one, because of the strong size dependence of λ. The reason for that is the phonon scattering at boundaries [32,76], which occurs when CNT length is smaller than the phonon mean path (about 1.5 μm [77]). In this work, though, we do not focus on the absolute values of thermal conductivity of CNTs, rather we intend to investigate the impact of geometry and chemical functionalizations (i.e. C–O–C tube interlinks) on λ.

Thermal conductivity of sole CNTs is affected by geometry (i.e. diameter, length, chirality and amount of layers) and chemistry (i.e. defects, vacations and functionalizations), as well as by their physical conditions (e.g. temperature). While the latter physical conditions are illustrated in other works [76], geometrical and chemical factors are of main interest here.

First of all, the effect of the tube diameter on λ is evaluated for 10 nm long SWCNTs, by choosing values ranging from 0.7 up to 5.0 nm. Fig. 4a shows that thermal conductivity scales linearly with the diameter D in the considered interval (fitting parameters: $k_1 = 3.0$ W m^{-1} K^{-1} nm^{-1} and $k_2 = 73.5$ W m^{-1} K^{-1}; coefficient of determination: $R^2 = 0.99$), namely from 75 W m^{-1} K^{-1} ($D = 0.7$ nm) to 88 W m^{-1} K^{-1} ($D = 5.0$ nm). Despite the fact that there is no general agreement in the literature on the effect of CNT diameter on λ [14], the relationship $\lambda \sim D$ is for example also found by Qiu et al. [78]. The concurrent decrease of phonon scattering and increase of conduction channels with tube diameter may provide an explanation of the above slight direct proportionality. However, if the CNT cross-sectional area is evaluated as $S = \pi r^2$ instead of $S = 2\pi rb$, the $D-\lambda$ relation changes as $\lambda \sim 1/D$; whereas thermal transmittance $U \sim \lambda S$ increases with CNT diameter in both cases.

Moreover, the effect of CNT length is assessed by considering (5,5) SWCNTs 10–40 nm long. Results range from 75 ($L = 10$ nm) to 186 W m^{-1} K^{-1} ($L = 40$ nm). Trend in Fig. 4b suggests that $\lambda \sim L^{\alpha}$ (fitting parameters: $k_3 = 19.2$ W m^{-1} K^{-1} nm$^{-\alpha}$ and $\alpha = 0.62$; coefficient of determination: $R^2 = 0.99$), where α is in good agreement with other works [32]. Therefore, the increase in the tube length has a significant effect on λ: In the ballistic regime, longer CNTs also present vibrational modes with longer wavelengths, which add new pathways for phononic heat transfer not experienced in the shorter ones.

The effect of chirality on λ is evaluated by testing CNTs with $D \cong 4.5$ nm and different chirality ((33,33) armchair; (43,23) chiral and (57,0) zigzag) as well as $D \cong 5.0$ nm ((37,37) armchair; (47,27) chiral and (64,0) zigzag), being the length fixed at 20 nm. Results in Fig. 4c show that armchair and chiral CNTs have similar λ (average difference below 1%), whereas zigzag CNTs have a slightly lower λ than armchair and chiral ones (about 15% less). Note that the $\lambda \sim D$ trend is confirmed. While a similar proportionality is also found in other works [79], in literature there is no general consensus on effect of chirality on λ. However, phonon density of states is almost not influenced by CNT chirality [80], which also means that chirality has a negligible effect on λ.

Thermal conductivities of SWCNTs are compared to thermal conductivities of CNTs with same length, chirality and diameter but being part of DWCNTs, as inner or outer tubes. The analyzed cases are (from left to right in Fig. 4d): 10 nm long (5,5) SWCNT vs. inner tube of (5,5)(10,10) DWCNT; 10 nm long (10,10) SWCNT vs. outer tube of (5,5)(10,10) DWCNT; 20 nm long (37,37) SWCNT vs. outer tube of (33,33)(37,37) DWCNT; 20 nm long (47,27) SWCNT vs. outer tube of (43,23)(47,27) DWCNT; 20 nm long (64,0) SWCNT vs. outer tube of (57,0)(64,0) DWCNT. As evident in Fig. 4d, a general slight increase in λ (about 20% more in average) is noticeable when the CNT is part of a DWCNT, regardless of the fact that it is the inner or the outer tube. To our knowledge, this effect has never been reported before. However, the observed trend may be due to the stress induced on the inner/outer DWCNT tubes by reciprocal Van der Waals interactions, which has been demonstrated to enhance λ [81].

Once geometrical effects on λ are explored, other simulations have been performed for estimating the thermal conductivity of chemically functionalized SWCNTs. In this case, parallel overlapping CNTs, covalently bonded each other by a variable number of C–O–C joints, are considered (see Fig. 1e). To this purpose, as shown in Fig. 1c, carbon rings are thermostated (green dotted area)

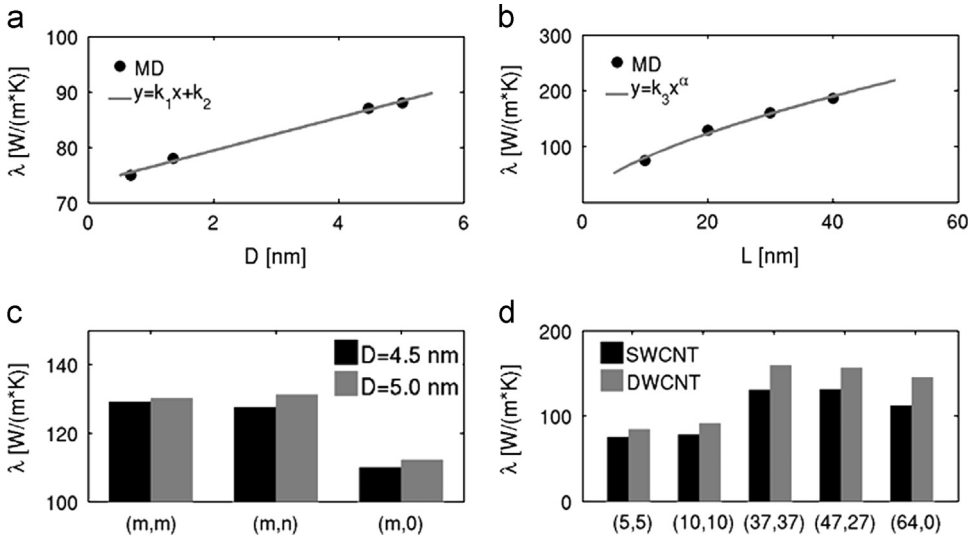

Fig. 4. Effect of CNTs geometry on thermal conductivity: (a) effect of SWCNT diameter; (b) effect of SWCNT length; (c) effect of SWCNT chirality; and (d) comparison between thermal conductivities of CNTs in single-walled or double-walled configurations.

at the ends of the lower (5,5) SWCNT ($L=10$ nm, with an overlap between the two jointed SWCNT of 2.5 nm along the CNT axis), in order to extract temperature profile and heat flux between the thermostats. Cases with 0, 1 and 4 C–O–C joints are considered, and the resulting λ are 76, 60 and 60 W m^{-1} K^{-1}, respectively. Again, λ is 75 W m^{-1} K^{-1} in the sole SWCNT case, as previously shown. Therefore, although λ of SWCNTs is not affected by overlap (case 0 joints); a significant drop in λ (about 20%) is found by adding one surface functionalization to SWCNT (case 1 joint). Moreover, the conductivity λ undergoes the same decrease by slightly varying the amount of functionalizations (case 4 joints).

As a matter of fact, Oxygen joints induce rehybridization of the functionalized carbon atoms, whose structure changes from sp^2 to sp^3. Hence, the presence of sp^3 carbons in the crystalline structure of CNT causes a localized phonon scattering, which reduces the phonon mean free path thus lowering λ up to 70%, according to the density of functionalizations [82]. Note that, the arrangement of defects has also a great importance in controlling λ: Once the first defect is introduced, patterned functionalizations with stripes parallel to heat flux (as our case) lower λ more gradually than perpendicular or random ones, while the amount of functionalizations is increased [83].

4.2. Thermal boundary resistance in carbon nanotube networks

The localized sources of thermal boundary resistance are identified in the simulated setups, which mimic the building blocks of more complex CNT network. R_k within and between DWCNTs is then evaluated, and the effect of CNT overlap and bonding compared.

In general, the thermal boundary resistance due to local phonon scattering is calculated as

$$R_k = \frac{\Delta T}{\varphi}, \tag{5}$$

where ΔT is the time averaged temperature discontinuity at the considered interface. Let us consider the geometry in Fig. 2d as representative of the building block of CNT networks: Thermal boundary resistances can be found between the layers of DWCNTs ($R_{k,1}$ and $R_{k,2}$, also known as intralayer Kapitza resistances) as well as between overlapping adjacent CNTs ($R_{k,12}$, also known as interlayer Kapitza resistance). In the first case ΔT refers to the time and space averaged temperature drop at steady state between inner and outer CNTs; while in the second case ΔT is the time and space averaged temperature drop at steady state between overlapping area of parallel CNTs. In both cases, φ is induced by the different temperatures of thermostats at the ends of the inner CNTs (Fig. 1c and d, red highlighted carbon rings). Note that a local temperature drop is also observed at the interface between thermostated and remaining carbon atoms; however, the corresponding R_k (about 2×10^{-11} m^2 K W^{-1}) can be 2–3 orders of magnitude lower than inter- or intralayer thermal boundary resistances and thus neglected [84].

First, $R_{k,1}$ and $R_{k,2}$ are evaluated within a pair of parallel (5,5) (10,10) 10 nm long DWCNTs with a 2.5 nm overlap and a number of joints ranging from 0 to 7 (Fig. 2d). While no significant change in the value of $R_{k,1}$ or $R_{k,2}$ is noticed by varying the amount of O-joints, $R_{k,2}$ (i.e. the Kapitza resistance within DWCNT with 280 K thermostat attached to the inner tube) is found to be slightly higher than $R_{k,1}$ (i.e. Kapitza resistance within DWCNT with 320 K thermostat attached to the inner tube), namely $(2.6\pm0.3$ s.d.$)\times 10^{-10}$ m^2 K W^{-1} and $(2.4\pm0.4$ s.d.$)\times 10^{-10}$ m^2 K W^{-1}, respectively. This difference is due to the inverse proportionality of R_k with temperature [85].

Second, the interlayer Kapitza resistance is studied by changing the overlap between SWCNTs and the amount of oxygen joints between adjacent SWCNTs or DWCNTs. The overlap effect on $R_{k,12}$ is investigated by varying the length of the overlapping region between two parallel (5,5) SWCNTs ($L=10$ nm both tubes; $h=0.23$ nm; $a=1$, 2.5, 5, 7.5 and 10 nm), as sketched in Fig. 5. $R_{k,12}$ is found to follow an exponential trend as a function of the overlap length (Fig. 5), ranging from 8.0×10^{-9} m^2 K W^{-1} ($a=1$ nm) to 1.3×10^{-9} m^2 K W^{-1} ($a=10$ nm), i.e. a 6-fold reduction, which can be fitted by

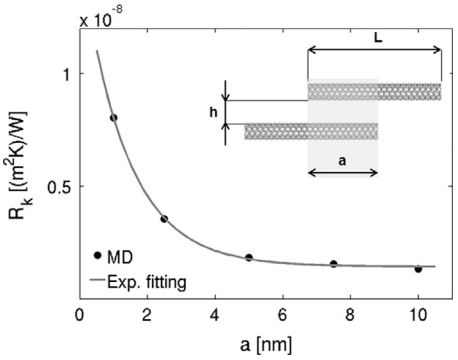

Fig. 5. Effect of the overlap a on the interlayer Kapitza resistance $R_{k,12}$ for a couple of parallel (5,5) SWCNTs.

$$R_k = \sum_i c_i\, e^{-\beta_i x} + R_k^0. \tag{6}$$

The asymptotic interlayer Kapitza resistance R_k^0 is found to be 1.4×10^{-9} m^2 K W^{-1}, and MD results are best fitted ($R^2>0.99$) by a single exponential decay (Eq. (6) with $i=1$, $x=a$, $c_1=13.9\times10^{-9}$ m^2 K W^{-1}, $\beta_1=0.7$ nm^{-1}). The remarkable decrease in $R_{k,12}$ is due to the increase of the available surface for heat transfer between the contiguous CNTs through van der Waals interactions. Even for different setups, similar reductions of $R_{k,12}$ with the increasing overlapping area between CNTs have been reported [84,86–88]. Moreover, previous experimental studies agree with the obtained $R_{k,12}$ values: For instance, Yang et al. report experimental thermal boundary resistances between MWCNTs around 1.0×10^{-9} m^2 K W^{-1} [89]. Finally, the effect on $R_{k,12}$ of adding covalent bonds between a couple of parallel (5,5) SWCNTs ($L=10$ nm in both tubes; $h=0.23$ nm; $a=2.5$ nm; number of joints=0, 1, 4, 8) or (5,5)(10,10) DWCNTs ($L=10$ nm in both tubes; $h=0.23$ nm; $a=2.5$ nm; number of joints=0, 1, 4, 7) is also investigated. In the SWCNTs setup in Fig. 6, ΔT_{0j} is the average temperature difference between the top and bottom tube in the overlapping area of the configuration with 0 joints; whereas ΔT_{4j} refers to the 4 joints case. In both cases, the interlayer Kapitza resistance $R_{k,12}$ is evaluated by means of Eq. (5) and using ΔT_{0j} and ΔT_{4j}, respectively. In the DWCNTs setup in Fig. 7, instead, bigger dots represent inner tubes (thermostats are attached at the tube ends) while smaller diamonds are representative of the outer tubes; as an example, ΔT_{in-out} is the average temperature difference between inner and outer tubes of top DWCNT in the 0 joints case, which allows to evaluate the intralayer Kapitza resistance $R_{k,1}$ by means of Eq. (5). As shown in Figs. 6 and 7, the introduction of C–O–C joints causes a decrease of the average temperature difference between contiguous SWCNTs or DWCNTs (e.g. $\Delta T_{4j}<\Delta T_{0j}$ if the SWCNTs case with 4 joints is compared to the 0 joints one, as depicted in Fig. 6) thus reducing significantly the value of $R_{k,12}$. If the SWCNTs setup (as shown in Fig. 2c) is considered, $R_{k,12}$ ranges from 3.6×10^{-9} m^2 K W^{-1} (0 joints) to 0.7×10^{-9} m^2 K W^{-1} (8 joints), i.e. a 5-fold reduction; whereas in the MWCNTs setup (as shown in Fig. 2d) $R_{k,12}$ ranges from 1.9×10^{-9} m^2 K W^{-1} (0 joints) to 0.4×10^{-9} m^2 K W^{-1} (8 joints), i.e. a 5-fold reduction. In both cases, $R_{k,12}$ shows an exponential decay by increasing the amount of joints (Fig. 8), which is again fitted with $R^2>0.99$ by Eq. (6), by considering $i=2$ (double

decaying exponential function with $c_1 = 2.0 \times 10^{-9}$ m^2 K W^{-1}, $\beta_1 = 4.7$, $c_2 = 1.0 \times 10^{-9}$ m^2 K W^{-1} and $\beta_2 = 0.3$ in case of SWCNTs; $c_1 = 1.1 \times 10^{-9}$ m^2 K W^{-1}, $\beta_1 = 2.3$, $c_2 = 0.7 \times 10^{-9}$ m^2 K W^{-1} and $\beta_2 = 0.1$ in case of DWCNTs) and x as the number of joints. The asymptotic interlayer Kapitza resistance R_k^0 (i.e. the minimum value of the Kapitza resistance achievable by adding a large amount of C–O–C joints between the CNTs) is found to be 0.5 $\times 10^{-9}$ m^2 K W^{-1} for SWCNTs, and 0.1×10^{-9} m^2 K W^{-1} for MWCNTs. The reported reduction in thermal boundary resistance is due to the supplementary bonded pathways – in addition to non-bonded ones – for carrying thermal vibrations (i.e. phonons) between adjacent CNTs. DWCNTs and SWCNTs show the same decaying exponential trend of $R_{k,12}$, but DWCNT's values are shifted down because of their larger contact area in this case (i.e. lower $R_{k,12}$ due to overlap effect), which gives rise to the observed offset. As in the above analysis on the overlap length, the decrease in $R_{k,12}$ due to the increase of the number of links between CNTs is in general agreement with both experimental [90,91] and modeling studies, even with different MD approaches and setups [57–60,92].

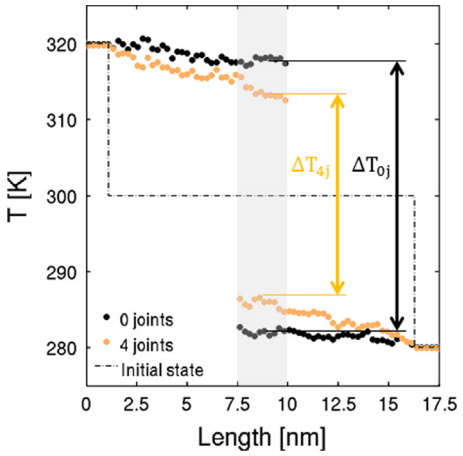

Fig. 6. Steady state temperature profiles of a pair of overlapping SWCNTs connected by 0 (black dots) or 4 (yellow dots) C–O–C covalent bonds (setup shown in Fig. 1c). (For interpretation of the references to color in this figure legend, the reader is referred to the web version of this article.)

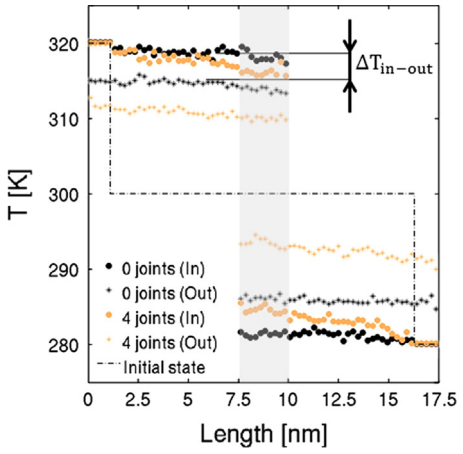

Fig. 7. Steady state temperature profile of a pair of overlapping DWCNTs connected by 0 (black dots) or 4 (yellow dots) C–O–C covalent bonds (setup shown in Fig. 1d). (For interpretation of the references to color in this figure legend, the reader is referred to the web version of this article.)

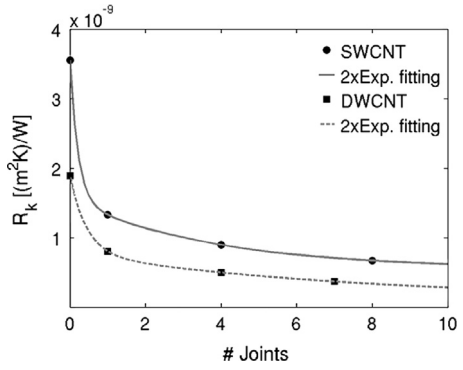

Fig. 8. Interlayer Kapitza resistance $R_{k,12}$ as a function of the number of C–O–C covalent bonds (i.e. joints) between a couple of parallel (5,5) SWCNTs or (5,5) (10,10) DWCNTs.

5. Discussion

According to the published results and the performed MD simulations, some key factors controlling thermal transmittance of CNT networks are highlighted.

First, CNTs should be a few hundreds of nanometer long, for allowing the existence of phonons with longer wavelengths thus increasing λ but avoiding technological problems such as structure stability and presence of impurities, which are typical for micrometer long CNTs.

Second, an ordered, parallel and partially overlapping arrangement of CNTs should be pursued within the network, though avoiding direct contact between CNTs, which causes defects in their crystalline structure and then a decrease of their internal λ [93]. Note that, because of the exponential decay governing the relation between R_k and the overlap length, even a short overlap is highly beneficial to the overall thermal transmittance.

Third, the introduction of a few short C–O–C joints between the CNTs constituting the carbon-based network significantly improves the thermal transmittance of the composite. As also noticed in other studies [59,60], short and stiff bonds (such as, C–O–C or C–CH_2–C) chemically affine to C–C should be preferred for reducing R_k, because of the corresponding shorter distance between CNTs, which allows a higher heat transfer via Van der Waals interactions, and the coupling of vibrational modes of the nanoconstructs within the network.

Therefore we would like to stress that, because of the decaying exponential trend of R_k with respect to the number of joints, even a single bonded interaction could be sufficient for a significant improvement of thermal transmittance.

Finally, the problem of finding a balanced number of bonded joints between CNTs is also addressed, because the functionalization of nanotubes disturbs pure sp^2 bonds thus inducing lower thermal conductivity. Therefore, when high thermal performances of CNT networks are demanded, the best design compromise between the introduction of functionalizations (i.e. phonon scattering sources) and the need for reducing the thermal boundary resistance is to add a limited amount of short joints between CNTs, chemically affine to C–C bonds. Hence, the quality and quantity of CNTs interlinks as well as the aligned and partially overlapping arrangement of CNTs appear to be crucial for improving thermal conductance of CNT networks and their composite materials, even at low filler content.

6. Conclusions

In this work, we have reviewed and provided numerical evidence of the impact of geometrical parameters and chemical functionalizations on the overall thermal transmittance in large complex

networks made up of carbon nanotubes (CNTs). The considered geometrical parameters are mainly dictated by the nanotube size, while functionalizations were implemented by the introduction of short C–O–C interlinks between two adjacent nanotubes.

For the sake of simplicity, we have focused on the *building blocks* of the above networks, so that the considered configurations consist of single and pairs of both single-walled carbon nanotubes (SWCNTs) and double-walled carbon nanotubes (DWCNTs) with different dimensions and number of interlinks.

We observed that as far as single tubes are concerned, diameter has a weak influence on the thermal conductivity λ, whereas a more significant impact is found instead for the length. Apart from secondary effects, the above conclusion also holds for each nanotube within a nanotube aggregate. In the latter case, high thermal boundary resistances (interlayer Kapitza resistance) are observed for contiguous nanotubes since the interaction between particles only relies upon secondary forces (van der Waals), and it exponentially decays to an asymptotic value by increasing the overlapping region. Moreover, a further reduction in the interlayer Kapitza resistance can be observed owing to the presence of interlinks between two nanotubes. Here, in particular, a double exponential decay proves to best fit the measured values. Our results show that few connections (two or three) are already sufficient to produce a significant improvement, while a further increase in the number of joints only produces a marginal reduction of the above resistance.

The present work may provide useful guidelines in designing the process for fabricating novel composite materials of great interest in modern thermal sciences, namely thermal storage and polymeric heat exchangers.

Conflict of interest

The authors declare no competing financial interests.

Acknowledgments

P.A. and E.C. acknowledge the support of the Italian Ministry of Research (FIRB Grant RBFR10VZUG) and the MITOR project (Surface coatings by carbon nanotubes for high heat transfer efficiency). P.A. and E.C. wish to thank Evelyn Wang and Sungwoo Yang from MIT for fruitful discussions. M.F. acknowledges travel support from the Scuola Interpolitecnica di Dottorato – SCUDO. Authors thank the CINECA (Iscra C project) and the Politecnico di Torino's DAUIN High Performance Computing Initiative for the availability of high performance computing resources and support.

References

[1] Serrano E, Rus G, García-Martínez J. Nanotechnology for sustainable energy. Renew Sustain Energy Rev 2009;13:2373–84.
[2] Trisaksri V, Wongwises S. Critical review of heat transfer characteristics of nanofluids. Renew Sustain Energy Rev 2007;11:512–23.
[3] Fraunhofer-Gesellschaft. Compact and flexible thermal storage. Res News, ⟨http://www.fraunhofer.de/en/press/research-news/2012/june/compact-and-flexible-thermal-storage.html⟩; 2012 [accessed 16.07.14].
[4] SAE-International. Adsorption-based thermal batteries could help boost EV range by 40%. SAE News, ⟨http://www.sae.org/mags/aei/12376⟩; 2014 [accessed 16.07.14].
[5] Chiavazzo E, Asinari P. Enhancing surface heat transfer by carbon nanofins: towards an alternative to nanofluids? Nanoscale Res Lett 2011;6:1–13.
[6] Huxtable ST, Cahill DG, Shenogin S, Xue L, Ozisik R, Barone P, et al. Interfacial heat flow in carbon nanotube suspensions. Nat Mater 2003;2:731–4.
[7] Chiavazzo E, Asinari P. Reconstruction and modeling of 3D percolation networks of carbon fillers in a polymer matrix. Int J Therm Sci 2010;49:2272–81.
[8] Han Z, Fina A. Thermal conductivity of carbon nanotubes and their polymer nanocomposites: a review. Prog Polym Sci 2011;36:914–44.
[9] McNamara AJ, Joshi Y, Zhang ZM. Characterization of nanostructured thermal interface materials – a review. Int J Therm Sci 2012;62:2–11.
[10] Clancy TC, Frankland SJV, Hinkley JA, Gates TS. Multiscale modeling of thermal conductivity of polymer/carbon nanocomposites. Int J Therm Sci 2010;49:1555–60.
[11] Iijima S. Helical microtubules of graphitic carbon. Nature 1991;354:56–8.
[12] Dresselhaus MS, Dresselhaus G, Charlier JC, Hernández E. Electronic, thermal and mechanical properties of carbon nanotubes. Philos Trans R Soc Lond Ser A: Math Phys Eng Sci 2004;362:2065–98.
[13] De Volder MF, Tawfick SH, Baughman RH, Hart AJ. Carbon nanotubes: present and future commercial applications. Science 2013;339:535–9.
[14] Marconnet AM, Panzer MA, Goodson KE. Thermal conduction phenomena in carbon nanotubes and related nanostructured materials. Rev Mod Phys 2013;85:1295–326.
[15] Samani MK, Khosravian N, Chen GCK, Shakerzadeh M, Baillargeat D, Tay BK. Thermal conductivity of individual multiwalled carbon nanotubes. Int J Therm Sci 2012;62:40–3.
[16] Chien S-K, Yang Y-T, Chen Co-K. The effects of vacancy defects and nitrogen doping on the thermal conductivity of armchair (10, 10) single-wall carbon nanotubes. Solid State Commun 2011;151:1004–8.
[17] Pan R, Xu Z, Zhu Z, Wang Z. Thermal conductivity of functionalized single-wall carbon nanotubes. Nanotechnology 2007;18:285704.
[18] Gulotty R, Castellino M, Jagdale P, Tagliaferro A, Balandin AA. Effects of functionalization on thermal properties of single-wall and multi-wall carbon nanotube–polymer nanocomposites. ACS Nano 2013;7:5114–21.
[19] Gardea F, Lagoudas DC. Characterization of electrical and thermal properties of carbon nanotube/epoxy composites. Compos Part B: Eng 2014;56:611–20.
[20] Worsley MA, Kucheyev SO, Satcher JJH, Hamza AV, Baumann TF. Mechanically robust and electrically conductive carbon nanotube foams. Appl Phys Lett 2009;94 (073115-3).
[21] Feng D, Feng Y, Zhang X. Numerical study of thermal conductivities of carbon-based mesoporous composites. Int J Thermophys 2014:1–16.
[22] Cheng H, Pez GP, Cooper AC. Spontaneous cross linking of small-diameter single-walled carbon nanotubes. Nano Lett 2003;3:585–7.
[23] Liu S, Shen Q, Cao Y, Gan L, Wang Z, Steigerwald ML, et al. Chemical functionalization of single-walled carbon nanotube field-effect transistors as switches and sensors. Coord Chem Rev 2010;254:1101–16.
[24] Weck PF, Kim E, Balakrishnan N, Cheng H, Yakobson BI. Designing carbon nanoframeworks tailored for hydrogen storage. Chem Phys Lett 2007;439:354–9.
[25] Won Y, Gao Y, Panzer MA, Dogbe S, Pan L, Kenny TW, et al. Mechanical characterization of aligned multi-walled carbon nanotube films using microfabricated resonators. Carbon 2012;50:347–55.
[26] Lee Y, Shanmugan S, Mutharasu D. Thermal resistance of CNTs-based thermal interface material for high power solid state device packages. Appl Phys A 2014;114:1145–52.
[27] Taphouse JH, Smith ONL, Marder SR, Cola BA. A pyrenylpropyl phosphonic acid surface modifier for mitigating the thermal resistance of carbon nanotube contacts. Adv Funct Mater 2014;24:465–71.
[28] Bhattacharya S, Amalraj R, Mahapatra S. Physics-based thermal conductivity model for metallic single-walled carbon nanotube interconnects. IEEE Electron Device Lett 2011;32:203–5.
[29] He S, Chen L, Xie C, Hu H, Chen S, Hanif M, et al. Supercapacitors based on 3D network of activated carbon nanowhiskers wrapped-on graphitized electrospun nanofibers. J Power Sources 2013;243:880–6.
[30] Cheng Z, Chai R, Ma P, Dai Y, Kang X, Lian H, et al. Multiwalled carbon nanotubes and NaYF4:Yb3+/Er3+ nanoparticle-doped bilayer hydrogel for concurrent NIR-triggered drug release and up-conversion luminescence tagging. Langmuir 2013;29:9573–80.
[31] Lee J, Kim YT, Spinks GM, Suh D, Lepró X, Lima MD, et al. All solid state carbon nanotube torsional and tensile artificial muscles. Nano Lett 2014;14:2664–9.
[32] Alaghemandi M, Algaer E, Böhm MC, Müller-Plathe F. The thermal conductivity and thermal rectification of carbon nanotubes studied using reverse non-equilibrium molecular dynamics simulations. Nanotechnology 2009;20:115704.
[33] Chang CW, Okawa D, Garcia H, Majumdar A, Zettl A. Nanotube phonon waveguide. Phys Rev Lett 2007;99:045901.
[34] Gordiz K, Allaei SMV. Thermal rectification in pristine-hydrogenated carbon nanotube junction: a molecular dynamics study. J Appl Phys 2014;115:163512.
[35] Jiang W, Ding G, Peng H. Measurement and model on thermal conductivities of carbon nanotube nanorefrigerants. Int J Therm Sci 2009;48:1108–15.
[36] Javadi FS, Saidur R, Kamalisarvestani M. Investigating performance improvement of solar collectors by using nanofluids. Renew Sustain Energy Rev 2013;28:232–45.
[37] Murshed S, Nieto de Castro C. Superior thermal features of carbon nanotubes-based nanofluids—a review. Renew Sustain Energy Rev 2014;37:155–67.
[38] Abdin Z, Alim MA, Saidur R, Islam MR, Rashmi W, Mekhilef S, et al. Solar energy harvesting with the application of nanotechnology. Renew Sustain Energy Rev 2013;26:837–52.
[39] Khodadadi JM, Fan L, Babaei H. Thermal conductivity enhancement of nanostructure-based colloidal suspensions utilized as phase change materials for thermal energy storage: a review. Renew Sustain Energy Rev 2013;24:418–44.
[40] Jänchen J, Ackermann D, Stach H, Brösicke W. Studies of the water adsorption on Zeolites and modified mesoporous materials for seasonal storage of solar heat. Sol Energy 2004;76:339–44.
[41] Bui K, Grady BP, Papavassiliou DV. Heat transfer in high volume fraction CNT nanocomposites: effects of inter-nanotube thermal resistance. Chem Phys Lett 2011;508:248–51.
[42] Gojny FH, Wichmann MHG, Fiedler B, Kinloch IA, Bauhofer W, Windle AH, et al. Evaluation and identification of electrical and thermal conduction mechanisms in carbon nanotube/epoxy composites. Polymer 2006;47:2036–45.

[43] Konatham D, Papavassiliou D, Striolo A. Thermal boundary resistance at the graphene–graphene interface estimated by molecular dynamics simulations. Chem Phys Lett 2012;527:47–50.
[44] Wang ZL, Mu HT, Liang JG, Tang DW. Thermal boundary resistance and temperature dependent phonon conduction in CNT array multilayer structure. Int J Therm Sci 2013;74:53–62.
[45] Balandin AA. Thermal properties of graphene and nanostructured carbon materials. Nat Mater 2011;10:569–81.
[46] Hayashi H, Takahashi K, Ikuta T, Nishiyama T, Takata Y, Zhang X. Direct evaluation of ballistic phonon transport in a multi-walled carbon nanotube. Appl Phys Lett 2014;104:113112.
[47] Murad S, Puri IK. Thermal transport through a fluid–solid interface. Chem Phys Lett 2009;476:267–70.
[48] Nanda J, Maranville C, Bollin SC, Sawall D, Ohtani H, Remillard JT, et al. Thermal conductivity of single-wall carbon nanotube dispersions: role of interfacial effects. J Phys Chem C 2007;112:654–8.
[49] Singh IV, Tanaka M, Endo M. Effect of interface on the thermal conductivity of carbon nanotube composites. Int J Therm Sci 2007;46:842–7.
[50] Yu A, Ramesh P, Sun X, Bekyarova E, Itkis ME, Haddon RC. Enhanced thermal conductivity in a hybrid graphite nanoplatelet–carbon nanotube filler for epoxy composites. Adv Mater 2008;20:4740–4.
[51] Sevik C, Sevinçli H, Cuniberti G, Çağın T. Phonon engineering in carbon nanotubes by controlling defect concentration. Nano Lett 2011;11:4971–7.
[52] Park J, Bifano MFP, Prakash V. Sensitivity of thermal conductivity of carbon nanotubes to defect concentrations and heat-treatment. J Appl Phys 2013;113 (034312-11).
[53] Gong F, Bui K, Papavassiliou DV, Duong HM. Thermal transport phenomena and limitations in heterogeneous polymer composites containing carbon nanotubes and inorganic nanoparticles. Carbon 2014;78:305–16.
[54] Vollebregt S, Banerjee S, Chiaramonti AN, Tichelaar FD, Beenakker K, Ishihara R. Dominant thermal boundary resistance in multi-walled carbon nanotube bundles fabricated at low temperature. J Appl Phys 2014;116:023514.
[55] Zhang J, Jiang C, Jiang D, Peng H-X. Nano-engineering thermal transport performance of carbon nanotube networks with polymer intercalation: a molecular dynamics study. Phys Chem Chem Phys 2014;16:4378–85.
[56] Choi SUS, Zhang ZG, Yu W, Lockwood FE, Grulke EA. Anomalous thermal conductivity enhancement in nanotube suspensions. Appl Phys Lett 2001;79:2252–4.
[57] Xu Z, Buehler MJ. Nanoengineering heat transfer performance at carbon nanotube interfaces. ACS Nano 2009;3:2767–75.
[58] Liu J, Alhashme M, Yang R. Thermal transport across carbon nanotubes connected by molecular linkers. Carbon 2012;50:1063–70.
[59] Varshney V, Lee J, Roy AK, Farmer BL. Modeling of interface thermal conductance in longitudinally connected carbon nanotube junctions. J Appl Phys 2011;109:084913–9.
[60] Varshney V, Patnaik SS, Roy AK, Farmer BL. Modeling of thermal conductance at transverse CNT – CNT interfaces. J Phys Chem C. 2010;114:16223–8.
[61] Lee JW, Meade AJ, Barrera EV, Templeton JA. Dependencies of the thermal conductivity of individual single-walled carbon nanotubes. Proc Inst Mech Eng Part N: J Nanoeng Nanosyst 2010;224:41–54.
[62] Chiavazzo E, Fasano M, Asinari P, Decuzzi P. Scaling behaviour for the water transport in nanoconfined geometries. Nat Commun 2014;5:4565.
[63] Cornell WD, Cieplak P, Bayly CI, Gould IR, Merz KM, Ferguson DM, et al. A second generation force field for the simulation of proteins, nucleic acids, and organic molecules. J Am Chem Soc 1995;117:5179–97.
[64] Quo Y, Karasawa N, Goddard WA. Prediction of fullerene packing in C60 and C70 crystals. Nature 1991;351:464–7.
[65] Walther JH, Jaffe R, Halicioglu T, Koumoutsakos P. Carbon nanotubes in water: structural characteristics and energetics. J Phys Chem B 2001;105:9980–7.
[66] Müller-Plathe F, Bordat P. Reverse non-equilibrium molecular dynamics. In: Karttunen M, Lukkarinen A, Vattulainen I, editors. Novel methods in soft matter simulations. Berlin Heidelberg: Springer; 2004. p. 310–26.
[67] Hoover WG. Canonical dynamics: equilibrium phase-space distributions. Phys Rev A 1985;31:1695–7.
[68] Nosé S. A unified formulation of the constant temperature molecular dynamics methods. J Chem Phys 1984;81:511.
[69] Shelly RA, Toprak K, Bayazitoglu Y. Nose–Hoover thermostat length effect on thermal conductivity of single wall carbon nanotubes. Int J Heat Mass Transf 2010;53:5884–7.
[70] Gordiz K, Allaei SMV, Kowsary F. Thermal rectification in multi-walled carbon nanotubes: a molecular dynamics study. Appl Phys Lett 2011;99:251901–4.
[71] Hess B, Kutzner C, van der Spoel D, Lindahl E. GROMACS 4: algorithms for highly efficient, load-balanced, and scalable molecular simulation. J Chem Theory Comput 2008;4:435–47.
[72] Pettersen EF, Goddard TD, Huang CC, Couch GS, Greenblatt DM, Meng EC, et al. UCSF Chimera—a visualization system for exploratory research and analysis. J Comput Chem 2004;25:1605–12.
[73] Son Y, Pal SK, Borca-Tasciuc T, Ajayan PM, Siegel RW. Thermal resistance of the native interface between vertically aligned multiwalled carbon nanotube arrays and their SiO_2/Si substrate. J Appl Phys 2008;103:024911–7.
[74] Cola BA, Xu J, Cheng C, Xu X, Fisher TS, Hu H. Photoacoustic characterization of carbon nanotube array thermal interfaces. J Appl Phys 2007;101:054313–9.
[75] Yao Z, Wang J-S, Li B, Liu G-R. Thermal conduction of carbon nanotubes using molecular dynamics. Phys Rev B 2005;71:085417.
[76] Lukes JR, Zhong H. Thermal conductivity of individual single-wall carbon nanotubes. J Heat Transf 2006;129:705–16.
[77] Hone J, Whitney M, Piskoti C, Zettl A. Thermal conductivity of single-walled carbon nanotubes. Phys Rev B 1999;59:R2514–6.
[78] Qiu B, Wang Y, Zhao Q, Ruan X. The effects of diameter and chirality on the thermal transport in free-standing and supported carbon-nanotubes. Appl Phys Lett 2012;100 (233105-4).
[79] Yan XH, Xiao Y, Li ZM. Effects of intertube coupling and tube chirality on thermal transport of carbon nanotubes. J Appl Phys 2006;99 (124305-4).
[80] Zhang G, Li B. Thermal conductivity of nanotubes revisited: effects of chirality, isotope impurity, tube length, and temperature. J Chem Phys 2005;123 (114714-114714).
[81] Abramson AR, Tien C-L, Majumdar A. Interface and strain effects on the thermal conductivity of heterostructures: a molecular dynamics study. J Heat Transf 2002;124:963–70.
[82] Ruiqin P, Zijian X, Zhiyuan Z, Zhenxia W. Thermal conductivity of functionalized single-wall carbon nanotubes. Nanotechnology 2007;18:285704.
[83] Pei Q-X, Sha Z-D, Zhang Y-W. A theoretical analysis of the thermal conductivity of hydrogenated graphene. Carbon 2011;49:4752–9.
[84] Zhong H, Lukes JR. Interfacial thermal resistance between carbon nanotubes: molecular dynamics simulations and analytical thermal modeling. Phys Rev B 2006;74:125403.
[85] Ong Z-Y, Pop E. Molecular dynamics simulation of thermal boundary conductance between carbon nanotubes and SiO_2. Phys Rev B 2010;81:155408.
[86] Evans WJ, Shen M, Keblinski P. Inter-tube thermal conductance in carbon nanotubes arrays and bundles: effects of contact area and pressure. Appl Phys Lett 2012;100 (261908-4).
[87] Hu G-J, Cao B-Y. Thermal resistance between crossed carbon nanotubes: molecular dynamics simulations and analytical modeling. J Appl Phys 2013;114:224308.
[88] Volkov AN, Salaway RN, Zhigilei LV. Atomistic simulations, mesoscopic modeling, and theoretical analysis of thermal conductivity of bundles composed of carbon nanotubes. J Appl Phys 2013;114:104301.
[89] Yang J, Waltermire S, Chen Y, Zinn AA, Xu TT, Li D. Contact thermal resistance between individual multiwall carbon nanotubes. Appl Phys Lett 2010;96 (023109-3).
[90] Kaur S, Raravikar N, Helms BA, Prasher R, Ogletree DF. Enhanced thermal transport at covalently functionalized carbon nanotube array interfaces. Nat Commun 2014;5:3082.
[91] Wang J, Chen D, Wallace J, Gigax J, Wang X, Shao L. Introducing thermally stable inter-tube defects to assist off-axial phonon transport in carbon nanotube films. Appl Phys Lett 2014;104:191902.
[92] Khare KS, Khabaz F, Khare R. Effect of carbon nanotube functionalization on mechanical and thermal properties of cross-linked epoxy–carbon nanotube nanocomposites: role of strengthening the interfacial interactions. ACS Appl Mater Interfaces 2014;6:6098–110.
[93] Aliev AE, Lima MH, Silverman EM, Baughman RH. Thermal conductivity of multi-walled carbon nanotube sheets: radiation losses and quenching of phonon modes. Nanotechnology 2010;21:035709.